Vacuum-Seal Waveguide Feedthrough for Extended W-Band 67-116 GHz

Citation for the original published paper (version of record):
Lapkin, I., López, C., Fredrixon, M. et al (2023). Vacuum-Seal Waveguide Feedthrough for Extended W-Band 67-116 GHz. IEEE Journal of Microwaves, 3(3): 1014-1018.
http://dx.doi.org/10.1109/JMW.2023.3279690

(article starts on next page)

IEEE Journal of Microwaves

Received 8 March 2023; revised 25 April 2023; accepted 17 May 2023. Date of publication 9 June 2023; date of current version 7 July 2023.

Digital Object Identifier 10.1109/JMW.2023.3279690

Vacuum-Seal Waveguide Feedthrough for Extended W-Band 67–116 GHz

IGOR LAPKIN, CRISTIAN LÓPEZ, MATHIAS FREDRIXON, ALEXEY PAVOLOTSKY, SVEN-ERIK FERM, VINCENT DESMARIS, AND VICTOR BELITSKY (Senior Member, IEEE)

Group for Advanced Receiver Development, Department of Space, Earth and Environmental Sciences, Chalmers University of Technology, SE-41296 Gothenburg, Sweden

CORRESPONDING AUTHOR: Victor Belitsky (e-mail: victor.belitsky@chalmers.se).

This work was supported by the European Sothern Observatory under Agreement 87603/ESO/18/88584/ASP.

ABSTRACT This article describes the design and performance of a vacuum-seal waveguide feedthrough with ultrawide RF band 67–116 GHz. We describe first the initial drivers behind the chosen design, then we present the results of the numerical simulations and optimization and provide thereafter the results of the RF and vacuum tests of the fabricated devices. The demonstrated RF performance is very close to the one expected from the simulation with an insertion loss less than 0.3 dB and a return loss better than 20 dB. Simultaneously, the feedthrough shows excellent vacuum isolation, Helium gas leak rate of $< 2\text{x}10^{-8}$ mbar·L/s is demonstrated, which allows using such a device in various space and ground applications.

INDEX TERMS Feedthrough, mm-waves, vacuum, waveguide.

I. INTRODUCTION

Different space and ground application at microwave and THz frequencies, involve temperature- or climate factors' sensitive equipment that should be placed into an isolated compartment or vacuum chamber, thus requiring interfacing via feedthroughs. In particular, modern communication technologies and instrumentation actively move to employ short mm-wave bands, creating the demand for wideband, low-loss, low-reflection vacuum-tight feedthroughs suitable for, e.g., moderate-power or low-signal instrumentation applications. This article describes the design and performance of a vacuum-seal waveguide feedthrough with ultrawide RF band 67–116 GHz referred as an extended W-band. In practice, the WR-10 waveguide interface of this feedthrough is used within an RF band significantly exceeding the specified WR-10 RF bandwidth of 75-110 GHz, reaching a fractional bandwidth of 54% of the central frequency.

Commercially available vacuum windows (or feedthroughs) for WR-10 waveguide have limited bandwidth by design, e.g., RF band 92–96 GHz, [1]. In such designs, a piece of solid dielectric, glass, quartz, etc., is typically brazed inside a length of a Kovar waveguide, which yields a helium leak rate of $< 10^{-8}$ mbar·L/s. However, the presence of a dielectric sealing element produces unwanted reflections and signal interferences between the two surfaces, i.e., vacuum-dielectric and dielectric-air separated by the length of the sealing dielectric. The interference between the reflected signals could be used to equalize the RF performance over a broader bandwidth [2]. Another common design uses a mica membrane placed between two waveguide flanges [3]. The sizes of such membrane are substantially larger than the waveguide dimensions thus possibly producing resonances within the operational RF band. Various designs have also been suggested for vacuum window or feedthrough [4]–[7]. However, none of these suggested designs combines a low insertion loss and a fractional bandwidth of 54%.

The vacuum-seal feedthrough presented in this article was designed for and intended to be used in a radio-astronomical receiver, ALMA Band 2 [8] with a required bandwidth of 67–116 GHz. The adopted specifications for this device were return loss better than 20 dB at any frequency within the band together with an insertion loss better than 0.3 dB averaged over the entire RF band. The helium leak rate requirement was specified at the level of $< 2.5\text{x}10^{-6}$ mbar·L/s after 20 minutes continuous exposure to the He gas and a lifetime of over 20 years.

II. FEEDTHROUGH DESIGN

Considering the difference of the pressure between the vacuum on one side of the waveguide window and atmosphere

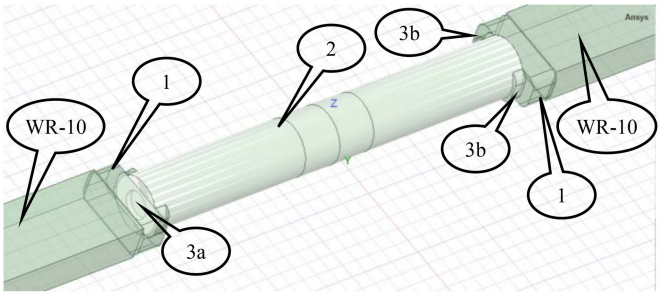

FIGURE 1. The feedthrough model used in the Ansys HFSS™. Input & output WR-10 waveguide sections; (1) matching sections with reduced-size rectangular waveguide with chamfered corners; (2) circular waveguide sealed with HDPE insert, (3a) and (3b) - elements of rectangular-to-circular transitions; (3a) points on the recess in the sealing HDPE insert while (3b) indicates positions for matching recesses in the circular waveguide. The transition layout is the same at both interfaces between the HDPE insert and the WR-10 waveguides.

on the other side, the WR-10 waveguide sealing is exposed to roughly 28 grams of the atmospheric pressure force at sea level. Potentially, this would open up for the usage of a very thin plastic membrane, e.g., thin Mylar film with a thickness of few tens of micrometers for adequate waveguide sealing. While it likely wouldn't produce unwanted resonances within the RF band, the long-term stability and especially the lifetime of such a solution is questionable. Furthermore, assuming an ultimately wide bandwidth of 67–116 GHz, a solution that could ensure single-mode propagation is preferred.

Foam materials, e.g., Rohacell, have lower dielectric constant and thus do not introduce strong discontinuity in the permittivity of material filling the waveguide. However, close-cell materials have the known drawback of potentially collapsing or irreversibly changing their shape after vacuum cycling. On the other hand, open-cell versions of such materials do not provide sufficient sealing and therefore cannot ensure long term compliance to the required leakage rate with 20-minutes He-exposure testing. Besides the cell size is quite comparable with the wavelength, which may lead to scattering or resonance effects and enhanced RF loss.

Assessing possible fabrication challenges, the sealing material should advantageously be introduced in a circular shallow structure (waveguide) to ensure tight press-fit tolerances towards all walls' surfaces that provide vacuum sealing. Furthermore, from an electromagnetic point of view the sealing material should be made of a dense material with low dielectric permittivity and RF loss, e.g., Teflon or high-density Polyethylene (HDPE), since their relatively low relative dielectric permittivity ($\varepsilon_r \sim 2 \ldots 2.5$) facilitates the RF matching at the sealing interfaces, insert/air and insert/vacuum. These materials are also known for their low RF dielectric loss with $\tan\delta$ of the order of $2\text{-}3\text{x}10^{-4}$ [9].

Summarizing the discussion above, the proposed novel waveguide feedthrough design for the ultra-wideband and low insertion loss operation employs the layout illustrated in Fig. 1. The input and output use a WR-10 rectangular waveguide, the sealing section employs a circular single-mode dielectric-filled waveguide. The matching sections connect the input / output WR-10 with the sealing section. The matching sections should not only effectively couple the rectangular WR-10 waveguides with their circular counterpart but also account for the changed propagation conditions in the dielectric of the sealing insert in the circular waveguide. HDPE was chosen as a material for the sealing insert, based on its better mechanical stability and long-term creep-free behavior under load as compared to Teflon.

III. MODELLING AND MECHANICS

An initial model for full 3D electromagnetic simulations using Ansys HFSS™ was built on fundamental assumptions for the waveguide geometry [10], and is shown in Fig. 1. The WR-10 standard interfaces came from the project requirements. In order to provide the required wideband operation, we opted for a two-step transition between the WR-10 waveguide and the circular waveguide sealing section.

The input and output rectangular waveguides made of standard WR-10 waveguide with the dimensions 1.27x2.54 mm^2, are followed by the roughly quarter-wavelength-long sections with slightly reduced transversal dimensions chamfered corners to 0.3 mm radius, to facilitate the fabrication by CNC milling machine (callout (1) in Fig. 1). In the HFSS™ model, these chamfered waveguide sections were set initially having standard WR-10 dimensions, which were free parameters for the optimization. The custom circular waveguide is filled with HDPE having a relative dielectric permittivity $\varepsilon_r = 2.37$, and $\tan\delta = 0.0003$ and has a diameter of 1.86 mm (callout (2) in Fig. 1). The dimensions (diameter) of the circular waveguide should allow propagation of the dominating TE_{11} mode above $F_L = 67$ GHz, lower edge of the RF band and preclude propagation of the second TM_{01} mode up to $F_U = 116$ GHz, the upper RF bandwidth frequency. Using equations from [10], we write the following conditions for the circular waveguide diameter, D:

$$D \geq \frac{1.841}{\pi \times F_L \times \sqrt{\mu\epsilon}} = 1.704\ mm \tag{1}$$

and

$$D \leq \frac{2.405}{\pi \times F_U \times \sqrt{\mu\epsilon}} = 1.979\ mm \tag{2}$$

The diameter of the circular waveguide for the sealing section, Fig. 1 callout (2), was chosen to be 1.86 mm fitting between the two limits given by (1) and (2). The HDPE insert become very flexible and difficult to handle during the pressing inside the metal parts of the feedthrough. For that purpose, we have chosen the diameter towards the upper limit defined by the (2) but with about 0.1 mm margin. A special tool was designed to facilitate pressing he HDPE insert that precludes bending.

The additional second step in the transition from the WR-10 to the circular waveguide, relies on edge modification of the circular waveguide, with small symmetric recesses at

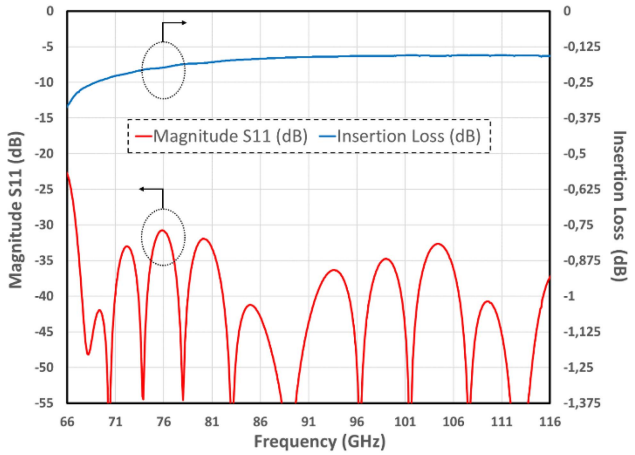

FIGURE 2. The Ansys HFSS™ simulated performance for the optimized feedthrough geometry. Blue curve displays the insertion loss vs. RF frequency, red curve shows the return loss at the input/output ports.

the sides, Fig. 1 callout (3b), and a coaxial recess in the HDPE insert, Fig. 1 callout (3a), of about a quarter of a wavelength at both ends. The recesses are also effectively changing the actual dielectric constant in the transition facilitating a reflection-free transition between the circular and rectangular waveguide sections of the feedthrough. The initial dimensions of the recesses were chosen to achieve a "filling factor" of the dielectric in this transition section such that $\epsilon_{eff} \sim 0.8x\sqrt{\epsilon_r}$. The initial feedthrough geometry model was further parametrized and the electrical performance was optimized in the Ansys HFSS™.

During the optimization, the overall length of the feedthrough remained constant, while the HDPE sealed circular waveguide dimensions were varied together with the dimensions of the matching elements of the transitions between the WR-10 rectangular waveguide and the circular sealing section. Fig. 2 displays the simulated performance of the proposed feedthrough for the model with the optimized dimensions.

The simulations for the optimized feedthrough were performed for the perfect geometry. For its practical implementation, the mechanical layout of the device should be constructed of two parts, Fig. 3(a). The main dimensions of the optimized feedthrough are given in Fig. 3(b). We used two O-rings in the design of the feedthrough. The internal O-ring (denoted as O2 in Fig. 3(a)) seals the split between the two metal halves and, by this, extends the effective isolating length of the HDPE insert into the air half of the feedthrough. The external O-ring (denoted as O1 in Fig. 3(a)) is used to seal the mounting interface of the feedthrough.

IV. TOLERANCE ANALYSIS

In order to define the manufacturing tolerances, we performed a sensitivity analysis of the design to mechanical fabrication accuracy using ANSYS HFSS™. In general, the alignment of the two halves of the feedthrough is provided by the dowel

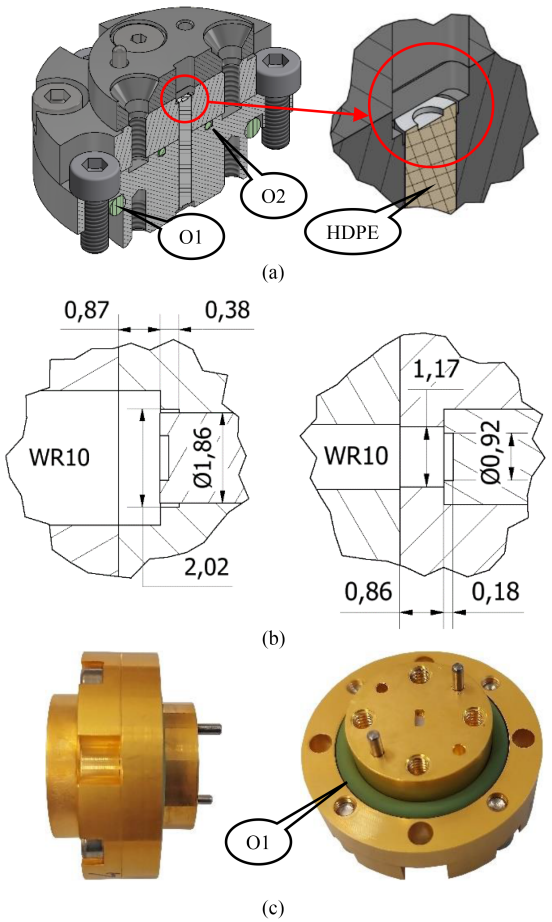

FIGURE 3. (a) 3D model of the feedthrough. Cross-section view of the feedthrough mechanical design with zoomed transition between the circular and rectangular waveguides. The HDPE sealing insert (14.3 mm long and 1.86 mm in diameter) is tightly constrained from both sides by the WR-10 sections. The callouts indicate position of the O-rings, O1 - the external O-ring and O2- the internal O-ring. (b) The main dimensions of the waveguide transition presented for two axial orthogonal cross-sections. (c) Fabricated feedthrough picture: the parts were made of aluminum alloy 6082-T65 and thereafter gold-plated.

pins with the pressing fit giving an estimated accuracy of the two parts alignment *better* than ±10 μm. Additionally, during the fabrication, we have used a special jig to align the opposite sides' interfaces of the feedthrough metal parts. The simulations of the lateral offset produced quite insignificant effect on the feedthrough performance for the allowed offsets, which is consistent with the results in [11].

The axial alignment of the two halves is naturally made by the pressing fit of the HDPE sealing insert. However, the rotational alignment by dowel pins at the interface between the two halves could allow some angular misalignment resulting into positioning the WR-10 input / output ports at some angle. From the point of view of the EM field propagation, it implies that the wave entering from the input WR-10 port and going through the polarization-neutral circular section hit the output WR-10 waveguide at some angle, leading inevitably to reflection and hence additional losses proportional to $cos(\alpha)$ where α is the misalignment angle.

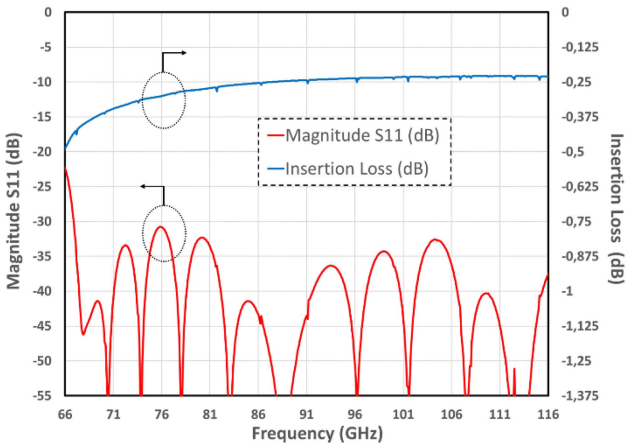

FIGURE 4. The Ansys HFSS™ simulated performance for the optimized feedthrough geometry and axial misalignment of $\alpha = 0.5$ degrees. The misalignment between the WR-10 input / output ports manifests itself by the suck-outs in the plot of the insertion loss and return loss vs. RF frequency.

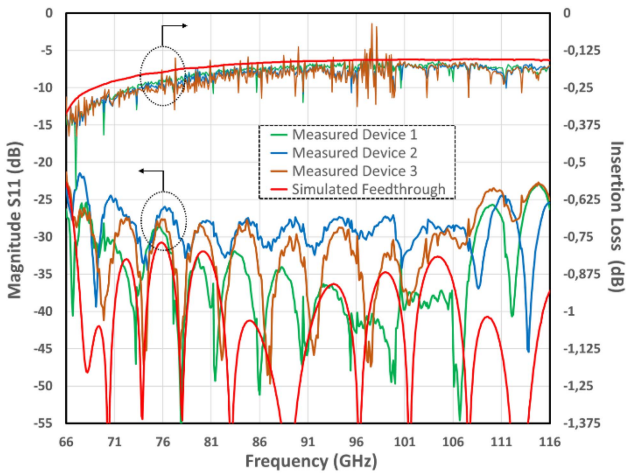

FIGURE 5. The measured RF performance of the three fabricated feedthroughs in comparison with simulations.The measurements were performed using VNA extension modules with the VNA set to 1 kHz IF bandwidth.

Such misalignment manifests itself by frequency suck-out in the insertion loss as presented in Fig. 4 for a misalignment angle of $\alpha = 0.5$ degrees.

V. MEASUREMENTS AND DISCUSSION

The performance of the fabricated feedthrough was measured using a Vector Network Analyzer (VNA), Keysight PNA-X, with frequency extension modules. To cover the extended W-band 67–116 GHz, two VNA waveguide extensions VDI WR-8 (90-140 GHz) and WR-10 (67-110 GHz) with corresponding waveguide adapters were used. The WR-10 extension module exhibits excessive noise that is manifested by small positive picks in the insertion loss plot especially at 97-99 GHz, Fig. 5.

The measurements were performed several times in order to obtain a reliable stitching between the results attained with the two different VNA extension modules. The presence of small amplitude suck-outs with max amplitude of ∼-0.11 dB at the measured insertion loss (Fig. 5) is likely to be ascribed to a small miss-alignment of the rectangular sections causing internal reflections and resonances, while the spread in return loss could be associated with a mixed effect of the small changes in the HDPE insert dielectric permittivity connected to the pressing and deformation during the assembling of the device and other small mechanical fabrication intolerances.

TABLE 1. Summary of the Performances for Feedthroughs

Ref.	S_{11}/S_{22}	S_{12}	RF band / Bandwidth*	Leak rate
[1]	18dB	-	92-96 GHz / 4.25%	-
[2]	~15dB	~0.5dB	70-110 GHz / 44.5%	~$1x10^{-7}$ mbar·L/s
[4]	~20dB	~0.3dB	24-38 GHz / 40%	~$1x10^{-6}$ mbar·L/s
[5]	~20dB	~4.3dB	75-105 GHz / 33%	$1.5x10^{-9}$ mbar·L/s
[6]	~7dB	>0.6dB	88-94 GHz / 6.7%	-
[7]	<20dB	<0.3dB	75-110 GHz / 38%	$5.4x10^{-7}$ mbar·L/s
This work	**<25dB**	**<0.3dB**	**67-116 GHz / 54%**	**$2x10^{-8}$ mbar·L/s****

* % of the central frequency, $(F_{max}+F_{min})/2$

** after continuous exposure to He gas for 20 minutes

The helium leak test was performed using the Pfeiffer Vacuum Technology GmbH SmartTest HLT560 leak detector. The vacuum-seal feedthrough was exposed to the Helium gas at atmospheric pressure continuously and a leak rate after 20 min exposure of less than $2x10^{-8}$ mbar·L/s has been measured, fully complying with the requirements to be below $2.5{\cdot}10^{-6}$ mbar·L/s.

Table 1 summarizes the performance of several feedthroughs available commercially or reported in the literature, showing that the superiority of our proposed design, when it comes to wideband vacuum-seal waveguide feedthrough operating in the W band.

VI. CONCLUSION

We presented a novel vacuum waveguide feedthrough that is rather tolerant to geometrical inaccuracies achieved by employing, e.g., standard fabrication by the CNC machining. The performance of the feedthrough was verified using RF and leak test measurements. The feedthrough demonstrated a low insertion loss below 0.3 dB and a return loss better than 20 dB over in the entire 67–116 GHz RF band corresponding to a fractional bandwidth of 54 %. In addition, the feedthrough has a leak rate better than $2x10^{-8}$ mbar·L/s. The design is relatively simple mechanically and could be scaled for other frequency band of interest and different applications. The feedthrough presented here was designed to be used in the ALMA Band 2 cold cartridge assembly [8].

ACKNOWLEDGMENT

We would like to thank our colleagues for useful discussions: J. Adema, J. Barkhof, R. Hesper, M. Bekema, A. Koops and M. Rodenhuis, NOVA NL; S. Ricciardi, R. Nesti, F. Cuttaia and F. Villa, INAF IT; N. Phillips and P. Yagoubov, ESO.

REFERENCES

[1] "WR-10 waveguide window model VWW-1107," CPI Beverly Microwave Division, Beverly MA 01915. [Online]. Available: https://www.cpii.com/product.cfm/8/1

[2] G. A. Ediss, N. Horner, F. Johnson, D. Koller, and A. R. Kerr, "WR-10 waveguide vacuum feedthrough for the ALMA Band-6 cartridge," ALMA Memo, 536, 2005.

[3] "WR-10 waveguide vacuum feedthrough," AeroWave Inc.

[4] H. Chen, S. Zheng, W. Che, Z. Luo, and Q. Xue, "A compact broadband transparent waveguide window based on low-loss cyclic olefin copolymer," *IEEE Microw. Wireless Compon. Lett.*, vol. 30, no. 4, pp. 335–338, Apr. 2020.

[5] C. Koenen et al., "A low-reflectivity vacuum window for rectangular hollow waveguides," *IEEE Trans. Microw. Theory Techn.*, vol. 66, no. 1, pp. 128–135, Jan. 2018.

[6] M. E. Hill, R. S. Callin, and D. H. Whittum, "High-power vacuum window in WR10," *IEEE Trans. Microw. Theory Techn.*, vol. 49, no. 5, pp. 994–995, May 2001.

[7] G. A. Kumar, S. Mondal, B. Biswas, and D. R. Poddar, "A broadband millimeter-wave waveguide window: A low-cost design for environmental protection," *IEEE Trans. Microw. Theory Techn.*, vol. 66, no. 10, pp. 4540–4547, Oct. 2018.

[8] V. Belitsky et al., "ALMA Band 2 Cold Cartridge Assembly Design," in *Proc. Int. Symp. Space THz Technol.*, 2022.

[9] J. W. Lamb, "Miscellaneous data on materials for millimetre and submillimetre optics," *Int. J. Infrared Millimeter Waves*, vol. 17, pp. 1997–2034, 1996, doi: 10.1007/BF02069487.

[10] D. M. Pozar, *Microwave Engineering*, 4th ed. Hoboken, NJ, USA: Wiley, 2011.

[11] A. R. Kerr, E. Wollack, and N. Horner, "Waveguide Flanges for ALMA Instrumentation," ALMA Memo No. 278, 1999.

IGOR LAPKIN received the M.Sc. degree from Technical State University, Nizhny Novgorod, Russia, in 1985. He is currently a Senior Researcher Engineer with the Group for Advanced Receiver Development, GARD, Department of Space, Earth, and Environmental Sciences, Chalmers University of Technology, Gothenburg, Sweden. His research interests include designing and developing components, mixers, and heterodyne receivers for radio astronomy.

CRISTIAN DANIEL LÓPEZ was born in Buenos Aires, Argentina, in 1990. He received the B.S. degree in electronic engineering from the Facultad de Ingeniería del Ejército Grl. Div. Manuel N. Savio, Buenos Aires, Argentina, in 2012, and the M.Sc. degree in microelectronics from the Universidad Politecnica de Cataluña, Barcelona, Spain, in 2018. He is currently working toward the Ph.D. degree with Chalmers University of Technology, Gothenburg, Sweden. His research focuses on the design and characterization of cryogenic components for THz systems.

MATHIAS FREDRIXON received the B.S. degree in engineering from Chalmers University of Technology, Gothenburg, Sweden. Since 1998, he has been with the Group for Advanced Receiver Development, GARD, Onsala Space Observatory, Chalmers University of Technology, Gothenburg, Sweden. He is currently a Senior Research Engineer and the main field is mechanical design and development of measuring systems and receivers for radio astronomy. He actively participated in developing ALMA Band five and Band two receivers, in development and support instruments for the APEX telescope in Chile, Swedish Odin satellite, and Hershel space telescope projects.

ALEXEY B. PAVOLOTSKY received the M.S. and Ph.D. degrees in material science and engineering from Moscow Aircraft Technology Institute/Technical University, Moscow, Russia, in 1990 and 2003, respectively. Since 2002, he has been with the Group for Advanced Receiver Development (GARD), Onsala Space Observatory, Chalmers University of Technology, Gothenburg, Sweden. He is currently holding a Senior Researcher position. His research interests include low-Tc superconducting thin film processing and characterization, and microfabrication in general.

SVEN-ERIK FERM started his work as a technician in 1995 participating in the Swedish Odin Satellite project with the Chalmers University of Technology, Gothenburg, Sweden. Since 2000, he has been with the Group for Advanced Receiver Development (GARD), Onsala Space Observatory, Chalmers University of Technology, Gothenburg, Sweden. He was with a camera manufacturer, Victor Hasselblad, for 15 years. Within the GARD group, he is responsible for manufacturing most fine mechanical parts.

VINCENT DESMARIS received the M.Sc. degree in material science from the National Institute of Applied Science, Lyon, France, in 1999, and the Ph.D. degree in electrical engineering from Chalmers University of Technology, Gothenburg, Sweden, in 2006. His thesis concerned the fabrication, characterization, and modeling of AlGaN/GaN microwave transistors. Since 2006, he has been with the Group for Advanced Receiver Development (GARD), Chalmers University of Technology and is currently the Head of GARD. His research interests include terahertz receiver technology, especially microfabrication and characterization of waveguide components and circuits and planar cryogenic microwave devices.

VICTOR BELITSKY (Senior Member, IEEE) received the M.Sc. degree in electrical engineering from Moscow Telecommunication Institute in 1977, and the Ph.D. degree in experimental physics from the Institute of Radio Engineering and Electronics, U.S.S.R. Academy of Sciences, Moscow, Russia, in 1990. He is currently a Professor with the Group for Advanced Receiver Development, Department of Space, Earth, and Environmental Sciences, Chalmers University of Technology, Gothenburg, Sweden. His research interests include terahertz and superconducting electronics and components, instrumentation for radio astronomy, and environmental science.